# MOLECULAR DOCKING ANALYSIS OF NOVEL THIOUREA DERIVATIVES OF NAPROXEN WITH POTENTIAL ANTITUMOR ACTIVITY

Nikola Nedeljkovic[1], Vladimir Dobricic[2], Marina Mijajlovic[1], Zorica Vujic[2] and Milos Nikolic[1]

[1]*University of Kragujevac, Faculty of Medical Sciences, Department of Pharmacy, Kragujevac, Serbia*
[2]*Department of Pharmaceutical Chemistry, University of Belgrade – Faculty of Pharmacy, Belgrade, Serbia*

Received: 17.05.2021.
Accepted: 23.08.2021.

**Corresponding author:**

**Milos Nikolic**

University of Kragujevac, Faculty of Medical Sciences, Kragujevac, Serbia, 69 Svetozara Markovica Street 34000 Kragujevac, Serbia

E-mail: milos.nikolic@medf.kg.ac.rs

sciendo

UDK: 616-006-074
Eabr 2023; 24(3):235-242
DOI: 10.2478/sjecr-2021-0037

## ABSTRACT

*Naproxen, as a propionic acid derivative, causes serious gastrointestinal side effects due to the presence of free carboxylic group. In that sense, masking of carboxylic group with other pharmacophores may be a promising strategy to decrease gastrointestinal toxicity. Thiourea derivatives have been intensively investigated as potential antitumor drugs, whereby their activity is based on potential inhibition of protein kinases, topoisomerases, carbonic anhydrase and sirtuins. In addition, it was shown that inhibition of certain protein kinases might reverse resistance to chemotherapeutic drugs by enhancing the cell death in the presence of low concentrations of drug. Twenty new thiourea derivatives of naproxen were designed and their binding to four selected protein kinases involved in tumor multidrug resistance (AKT2, mTOR, EGFR and VEGFR1) was estimated using two molecular docking programs (AutoDock Vina and OEDocking). According to OEDocking, the highest potential to inhibit AKT2 and mTor has derivative 1, while derivative 20 demonstrates the highest potential towards EGFR and VEGFR1. According to AutoDock Vina, the highest potential for inhibition of EGFR, AKT2 and VEGFR1 have derivatives 16 and 17. Therefore, derivatives 1, 16, 17 and 20 are potentially the most potent protein kinase inhibitors that could be further synthesized and tested for anticancer activity.*

***Keywords***: *Antitumor activity, AutoDock Vina, molecular docking, naproxen, thiourea derivatives.*

## INTRODUCTION

Naproxen is a non-steroidal anti-inflammatory drug which prevents conversion of arachidonic acid to eicosanoids through competitive inhibition of both cyclooxygenase isoenzymes (COX-1 and COX-2), resulting in analgesic and anti-inflammatory effects (1). As a propionic acid derivative, naproxen causes serious gastrointestinal side effects due to the presence of free carboxylic group (2). Therefore, masking carboxylic group with other moieties may be a promising strategy in order to decrease gastrointestinal toxicity (3). Piffar and coworkers showed that naproxen was able to reduce tumor growth in rats by 58% (4). Hydroxamic acid derivative of naproxen demonstrated histone deacetylase inhibition (5), while propanamide and urea derivatives showed cytotoxic effect against the cancer cell line HCT–116 (6).

Thiourea and other structure-related derivatives, such as thiosemicarbazones, have attracted great attention of scientists in terms of evaluation of their biological activity (7-9). The thiourea moiety has been described as an important pharmacophore in a variety of pharmacologically active compounds, including anti-inflammatory (10), antiviral (11), anticancer (12,13), hypoglycemic (14) and antimicrobial agents (15). In the past few decades, thiourea derivatives have been intensively investigated as potential anticancer drugs. This class of compounds has been recognized as agents with promising inhibitory activity towards human lung adenocarcinoma cell lines, human breast cancer cells and human colorectal carcinoma (16-18). Antitumor activity of thiourea derivatives is based on potential inhibition of protein kinases (19), topoisomerases (20), carbonic anhydrase (21) and sirtuins (22).

Protein kinases are widely studied targets in the drug design studies due to their pivotal role in regulation of cell functions (23). The activation of protein kinases in cell signaling pathways is associated with cancer cell survival, tumor invasiveness and drug resistance (24). Therefore, compounds targeting protein kinases have become one of the most studied classes of cytotoxic agents (25). Multidrug resistance (MDR) is a predominant cause of cancer chemotherapy failure, which is responsible for over 90% mortality of cancer (26,27). MDR can be associated with elevated metabolism and increased efflux of xenobiotics, growth factors, increased DNA (Deoxyribonucleic acid) repair capacity, and various genetic factors (28,29). It was also demonstrated that inhibition of certain protein kinases not only decreases the proliferation and growth of carcinoma cells, but may reverse resistance to chemotherapeutic drugs by enhancing the cell death in the presence of low concentrations of drug, thereby reducing drug side effects (30-33). Today, a number of biomedical studies are focused on design of antitumor drugs that are able to reverse MDR.

The aims of this study were to design new thiourea derivatives of naproxen and identify the most promising candidates that could be used for the therapy of MDR tumors. For this purpose, molecular docking analysis was carried out towards selected protein kinases involved in multidrug resistance in order to identify designed derivatives with the highest enzyme inhibitory activity.

## MATERIALS AND METHODS

### 2.1. Software

Geometry of designed compounds was optimized using Chem3D Ultra 7.0 (34). Preparation of ligands for the molecular docking calculations was carried out in AutoDockTools 1.5.6 (35) and OMEGA 2.5.1.4 (36,37). Protein molecules (selected protein kinases) were prepared for molecular docking in BIOVIA Discovery Studio Visualizer 17.2.0.16349 (38), AutoDockTools 1.5.6 and MAKE Receptor 3.2.0.2 software (39). AutoDock Vina (40) and OEDocking 3.2.0.2 software (41-43) were used for the analysis of binding poses and ligand-receptor interactions.

### 2.2. Designed compounds

Compounds designed and tested in this study (**1-20,** Figure 1) are thiourea derivatives of naproxen, containing amino acids glycine, L-alanine, β-alanine, L-valine and L-phenylalanine (**1-5**), their methyl (**6-10**) and ethyl (**11-15**) esters, as well as aromatic amines (**16-20**).

**Figure 1.** The structures of the tested compounds (1-20)

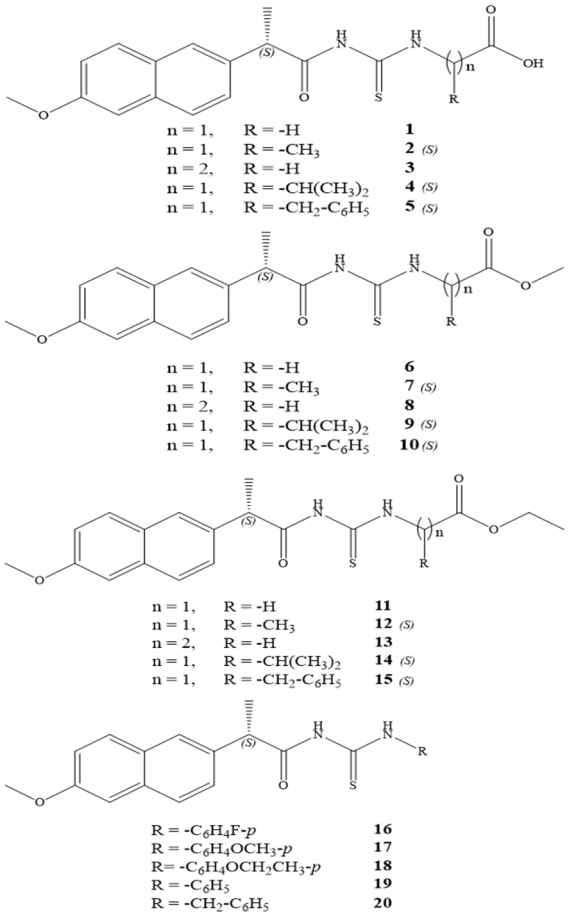

### 2.3. Ligand preparation

#### 2.3.1. AutoDock Vina

Geometry of tested molecules was optimized using AM1 semi-empirical quantum chemical methods in Chem3D Ultra 7.0 software. Furthermore, these molecules were imported into the Mercury 3.10.2 (44) and converted into the mol2 format. In order to prepare selected compounds for the docking calculations, AutoDockTools 1.5.6. was used to add Gasteiger charges, set rotatable bonds and save selected molecules in pdbqt format.

#### 2.3.2. OEDocking

Prior to the molecular docking in OEDocking 3.2.0.2, ligand preparation was performed in OMEGA 2.5.1.4 and files containing 200 conformers for each ligand were generated.

### 2.4. Selection and preparation of receptors

Crystal structures of four protein kinases involved in multidrug resistance were taken from the Protein Data Bank (45): 1M17 (Epidermal Growth Factor Receptor - EGFR), 3E87 (RAC-beta serine/threonine-protein kinase - AKT2), 3HNG (Vascular endothelial growth factor receptor 1 - VEGFR1) and 4JSV (Serine/threonine-protein kinase - mTOR). Details of selected enzymes were presented in Table 1.

#### 2.4.1. AutoDock Vina

BIOVIA Discovery Studio Visualizer v. 17.2.0.16349 was used to remove the co-crystalized ligands, water molecules and unnecessary receptor chains. Prior to docking, AutoDockTools 1.5.6. was used to prepare the proteins for AutoDock Vina by assigning hydrogens and converting protein structures from pdb to pdbqt format.

**Table 1.** Protein kinases selected for this study

| Target | Selected PDB (resolution) | Co-crystalized ligand | Chains | Selected chain |
|---|---|---|---|---|
| EGFR | 1M17 (2.60 Å) | [6,7-*bis*(2-methoxy-ethoxy)quinazoline-4-yl]-(3-ethynylphenyl)amine (Ligand ID: **AQ4**) | A | A |
| AKT2 | 3E87 (2.30 Å) | *N*-[(1*S*)-2-amino-1-phenylethyl]-5-(1*H*-pyrrolo[2,3-*b*]pyridin-4-yl)thiophene-2-carboxamide (Ligand ID: **G95**) | A, B | A |
| VEGFR1 | 3HNG (2.70 Å) | *N*-(4-chlorophenyl)-2-[(pyridin-4-ylmethyl)amino]benzamide (Ligand ID: **8ST**) | A | A |
| mTOR | 4JSV (3.50 Å) | adenosine-5'-diphosphate (Ligand ID: **ADP**) | A, B | A |

Based on the location coordinates of the co-crystalized ligand AQ4 in the 1M17 crystal structure, which were set to x = 21.697, y = 0.303 and z = 52.093, a grid box of 42, 16, and 20 points in x-, y-, and z-direction, respectively, with grid spacing of 0.375 Å was built and centered on the co-crystalized ligand. The location coordinates of native G95 ligand in the 3E87 crystal structure were x = 33.914, y = -14.631 and z = 7.695 and based on that, a grid box of 26, 32, and 24 points was built and centered on the co-crystalized ligand. The coordinates of the co-crystalized ligand 8ST in the 3HNG crystal structure were x = 3.911, y = 17.995 and z = 32.857, while grid box size was set to x = 22, y = 32 and z = 30. Finally, the location coordinates of ADP ligand in the 4JSV crystal structure were x = 50.115, y = -1.981 and z = -45.385, while grid box size was set to x = 30, y = 18 and z = 32.

#### 2.4.2. OEDocking

The receptor sites for molecular docking in OpenEye were prepared using MAKE Receptor 3.2.0.2 software (39). The outer contour sizes were 1017 $Å^3$ (EGFR), 598 $Å^3$ (AKT2), 493 $Å^3$ (VEGFR1) and 2150 $Å^3$ (mTOR), while the grid box sizes were 6416 $Å^3$ (EGFR), 5974 $Å^3$ (AKT2), 6314 $Å^3$ (VEGFR1) and 5190 $Å^3$ (mTOR). The setup of contours was set as "Balanced" and for the docking of ligands into AKT2 following constraints were added: Glu230 as a hydrogen bond donor and Ala232 as a hydrogen bond acceptor.

### 2.5. Molecular docking

#### 2.5.1. AutoDock Vina

Molecular docking calculations were performed in AutoDock Vina software (40) with the default scoring function. In this docking simulation, semi-flexible docking protocols in which the target protein was kept as rigid were used. Maximum of nine poses were generated for the each tested compound.

#### 2.5.2. OEDocking

The OEDocking 3.2.0.2 software (41-43), which employs FRED (fast exhaustive docking) tool, was also used for the analysis of ligand binding poses into the defined receptor sites of tested enzymes. Exhaustive scoring was performed using Chemgauss4 scoring function. Further optimization was done using OEChemscore scoring function. Scoring and consensus pose selection were performed using Chemgauss4 scoring function. Other settings were set as default.

#### 2.5.3. Validation of docking methodology

For the docking validation, the co-crystalized ligands were extracted and re-docked into the active sites of the target enzymes. Binding poses were compared with the conformations of co-crystalized ligands and root-mean-square deviation (RMSD) values were calculated. In the molecular docking study, *in silico* prediction is considered successful if the RMSD value is less than 2.0 Å for the best scored conformation (46).

## RESULTS

### 3.1. Validation of Molecular Docking

For the evaluation of molecular docking results validity, the co-crystalized ligand has to be re-docked into the active site. RMSD value was calculated by superimposition of native and re-docked co-crystalized ligand conformations using BIOVIA Discovery Studio Visualizer. Calculated RMSD values were < 2 Å in all docking experiments.

### 3.2. Molecular docking analysis

Tables 2 and 3 summarize the binding parameters of the molecules with highest binding potential against selected protein kinases in AutoDock Vina and OEDocking. Binding parameters include docking score, as well as the type and number of the key binding interactions. Only those interactions that both co-crystalized ligands and tested molecules form with receptors are listed in these tables.

**Table 2.** An overview of the key binding interactions and docking scores of the top scored compounds in AutoDock Vina

| Designed ligand number | PDB code | Hydrogen bonds | Other interactions | Docking score (kcal/mol) | |
|---|---|---|---|---|---|
| | | | | Designed ligand | Co-crystalized ligand |
| 16 | 1M17 | - | Leu694, Leu820, Asp831, Ala719 | -8.7 | -7.2 |
| | 3E87 | Asp293 | Ala179, Leu158, Val166, Phe163, Met282 | -9.0 | -8.9 |
| | 3HNG | Glu878, Asp1040 | Val841, Val892, Ala859, Leu1029, Lys861, Val909, Cys912, Phe1041 | -10.9 | -10.5 |
| 17 | 1M17 | - | Ala719, Thr766, Leu820, Asp831 | -8.7 | -7.4 |
| | 3E87 | Asp293 | Ala179, Val166, Lys181, Phe163, Met282 | -8.5 | -8.8 |
| | 3HNG | Glu878, Asp1040 | Val841, Val892, Ala859, Leu1029, Lys861, Val909, Cys912, Phe1041 | -10.7 | -10.2 |

**Table 3.** An overview of the key binding interactions and docking scores of the top scored compounds in OEDocking

| Designed ligand number | PDB code | Hydrogen bonds | Other interactions | Docking score (kcal/mol) | |
|---|---|---|---|---|---|
| | | | | Designed ligand | Co-crystalized ligand |
| 1 | 3E87 | Glu230, Ala232 | Val166, Leu158, Glu279, Asp293, Phe439 | -9.48 | -15.20 |
| | 4JSV | Lys2187 | Glu2190, Pro2169, Leu2185, Ile2356 | -7.52 | -9.43 |
| 20 | 1M17 | Met769 | Thr766, Met742, Ala719, Lys721, Leu694, Val702, Cys773, Asp831 | -9,63 | -10.49 |
| | 3HNG | Glu878, Asp1040 | Cys1018, Leu1013, Leu882, Val891, Val909, Val892, Val841, Phe1041, Ala859, Leu1029, Ile885 | -11.8 | -14.60 |

Molecular docking analysis in AutoDock Vina software revealed that derivatives **16** and **17** bound to EGFR, AKT2 and VEGFR1 similarly to the corresponding co-crystalized ligands. On the other hand, in the OEDocking software the best docking scores and presence of the key binding interactions were observed for derivatives **1** (AKT2 and mTOR) and **20** (EGFR and VEGFR1).

## DISCUSSION

Multidrug resistance (MDR) is one of the major challenges in cancer treatment and may result in cross-resistance to many other structurally different chemotherapeutics. Antitumor activity of thiourea derivatives has been established earlier in numerous studies (12,13). Preliminary *in silico* studies can facilitate the rapid discovery of novel antitumor drugs which are able to reverse MDR. To identify suitable antitumor agents from the designed compounds, the molecular docking study was carried out towards selected protein kinases involved in MDR.

Co-crystalized molecules AQ4, G95, 8ST and ADP (Adenosine diphosphate) are ligand molecules isolated from the crystal structures 1M17, 3E87, 3HNG and 4JSV (co-crystalized ligands). Interactions between co-crystalized ligands and corresponding enzymes are considered key binding interactions. Type and number of key binding interactions, as well as docking scores were main parameters for assessing the potential of designed compounds to inhibit selected protein kinases.

Docking visualization is presented as 2D and 3D view of the key binding interactions. In order to achieve visibility of the docked ligand into the protein structure, ligands were shown as blue color sticks in the binding pocket of the protein, shown as green surface.

The OEDocking and AutoDock Vina software were used for the binding mode analysis of tested compounds into the active sites of selected protein kinases. According to OEDocking, top scored derivatives were 1 (towards AKT2 and mTOR) and 20 (towards EGFR and VEGFR1). On the other hand, in AutoDock Vina top scored derivatives were 16 and 17 (towards EGFR, AKT2 and VEGFR1). The binding modes of these four derivatives will be further discussed in details.

Derivatives 16, 17 and 20 bound to EGFR with lower binding energies compared to the co-crystalized ligand. Nitrogen atoms of erlotinib quinazoline ring formed two hydrogen bonds with Met769 and Gln767, while the phenyl moiety of quinazoline formed π-sigma interaction with Leu694. The ethynylphenyl moiety formed π-cation interaction with Lys721 and hydrophobic interaction with Ile720, Ala719, Ile765, Lue764, Thr766 and Thr830 (47). Derivatives with the best docking results in AutoDock Vina did not accomplish any key hydrogen bond interactions, but formed four hydrophobic interactions each. On the other hand, derivative 20 formed an identical hydrogen bond with Met769 residue as erlotinib. Similar hydrophobic interactions with residues Thr766 and Ala719 were observed during the binding of *N*-allylthiourea derivatives into the EGFR active site (48).

In the active site of AKT2, co-crystalized nitrogen atoms of 1*H*-pyrrolo[2,3-*b*]pyridin-4-yl moiety formed two hydrogen bonds with Glu230 and Ala232, while phenylethyl moiety formed one weak carbon-hydrogen bond with Asp293 residue (49). Despite significantly higher binding energy of derivative 1 in comparison to the co-crystalized ligand, this derivative formed two hydrogen bonds with Glu230 and Ala232 (Figure 2). In contrast, derivatives 16 and 17 formed only one conventional hydrogen bond with residue Asp293, although they were bound with very similar binding energy in comparison to the co-crystalized ligand.

**Figure 2.** Compound 1 docked into the active site of AKT2.

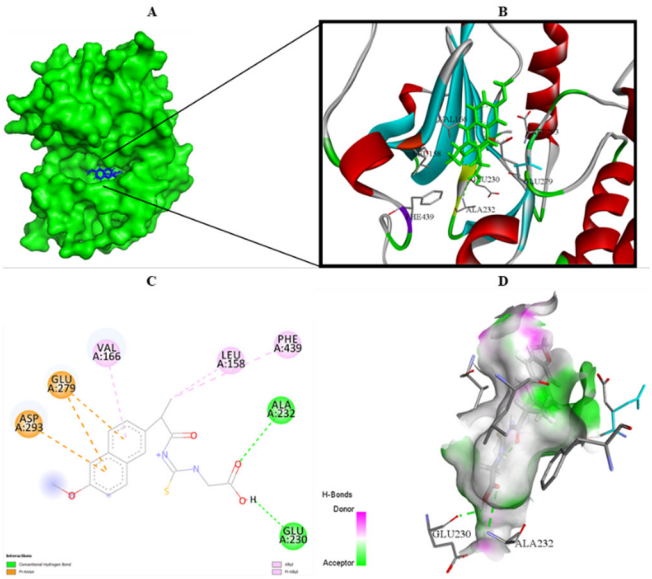


A) Best ligand conformation in the binding pocket of the enzyme. B) and C) 2D and 3D summary views of all binding interactions achieved by compound **1** into the active site of AKT2 (hydrogen bonds were presented as green dash lines). D) 3D visualization of hydrogen bond donors and acceptors distribution of this compound.

Binding score values indicate that derivatives **16**, **17** and **20** bound to the VEGFR1 with highest affinity compared to other target proteins, achieving the largest number of key binding interactions. Above-mentioned compounds formed two identical hydrogen bonds with residues Glu878 and Asp1040. On the other hand, derivative **1** formed the same hydrogen bond with Asp1040 and one different key hydrogen bond interaction with Cys912. The amino acid residues involved in the formation of key binding interactions between the best docked derivatives and active site of VEGFR1 are illustrated in the Figures 3, 4 and 5.

**Figure 3.** Compound 16 docked into the active site of VEGFR1.

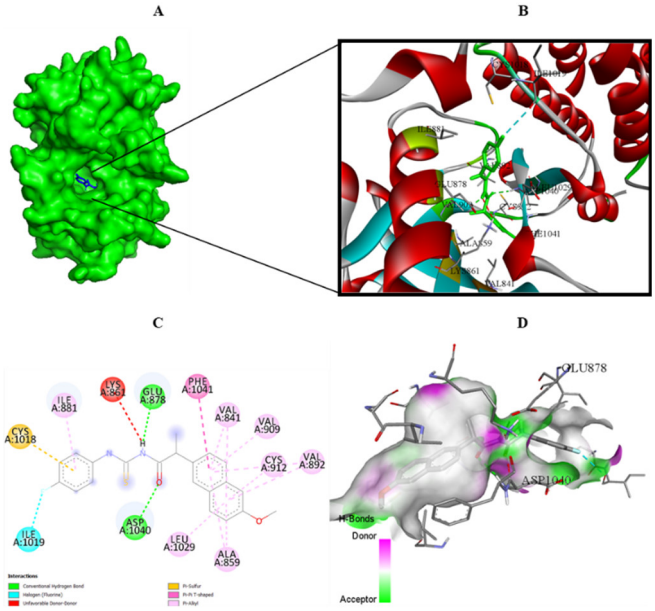


A) Best ligand conformation in the binding pocket of the enzyme. B) and C) 2D and 3D summary views of all binding interactions achieved by compound **16** into the active site of VEGFR1 (hydrogen bonds were presented as green dash lines). D) 3D visualization of hydrogen bond donors and acceptors distribution of this compound.

**Figure 4.** Compound **17** docked into the active site of VEGFR1.

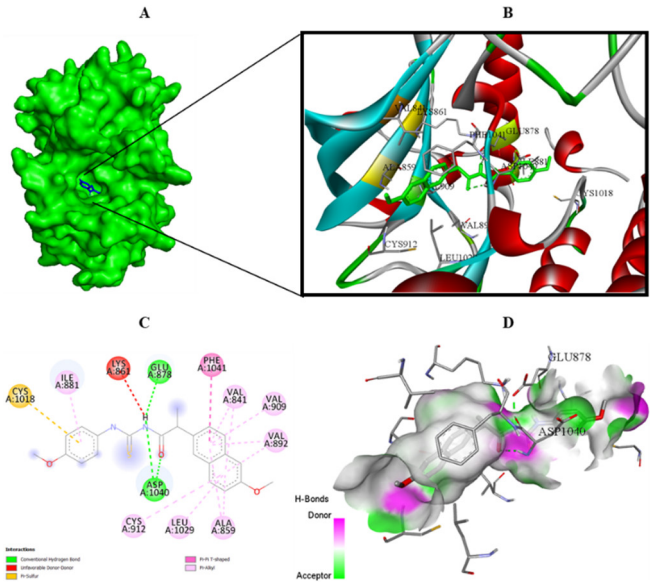


A) Best ligand conformation in the binding pocket of the enzyme. B) and C) 2D and 3D summary views of all binding interactions achieved by compound **17** into the active site of VEGFR1 (hydrogen bonds were presented as green dash lines). D) 3D visualization of hydrogen bond donors and acceptors distribution of this compound.

**Figure 5**. Compound 20 docked into the active site of VEGFR1.

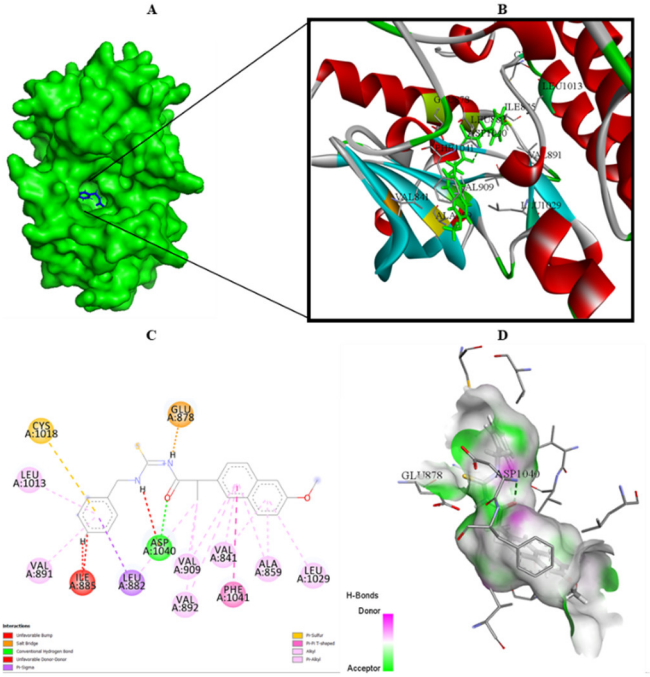


A) Best ligand conformation in the binding pocket of the enzyme. B) and C) 2D and 3D summary views of all binding interactions achieved by compound **20** into the active site of VEGFR1 (hydrogen bonds were presented as green dash lines). D) 3D visualization of hydrogen bond donors and acceptors distribution of this compound.

Designed compound **1** demonstrated lower binding score towards mTOR compared to the co-crystalized ADP ligand. ADP in mTOR formed three hydrogen bonds with residues Lys2187, Val2240 and Asp2357 and also seven Van der Waals interactions (50). In the active site of mTOR, derivative **1** accomplished a hydrogen bond with Lys2187 and four significant hydrophobic interactions.

Two the most critical components for a docking program are sampling algorithm and scoring function, which determine its sampling and scoring power. AutoDock Vina generates different ligands conformers using a quasi-Newton Broyden-Fletcher-Goldfarb-Shanno (BFGS) search algorithm. BFGS uses scoring function with respect to the position, orientation and torsions of the ligand. The Vina scoring function is fully empirical including Gaussian steric interactions, repulsion, hydrogen bonds, hydrophobic and torsion terms. On the other hand, the OEDocking software employs fast exhaustive docking that docks molecules using an exhaustive search algorithm. During the exhaustive search, unrealistic poses are filtered and retained ones are scored. The best scoring pose is used to rank the ligand against other ligands in the screening database. Chemgauss4 is default scoring function used by FRED that employs Gaussian-smoothed potentials to measure the complementarity of ligand poses within the active site.

AutoDock Vina and OEDocking estimated various binding affinity of the same ligands towards selected protein kinases. Due to different scoring functions and search algorithms of these two docking programs, the obtained binding parameters may be diverse even for the same protein-ligand complex. Although top scored derivatives in these two docking programs are different (**1** and **20** in OEDocking, **16** and **17** in AutoDock Vina), it can be noticed that according to OEDocking derivative **17** had lower binding score than derivatives **1** and **20,** but formed some of the key binding interactions with mTOR and EGFR. Therefore, derivative **17** also has potential to inhibit these enzymes. Similarly, according to AutoDock Vina, derivative **1** had binding scores similar to binding scores of **16** and **17** and formed some of the key binding interactions with AKT2 and VEGFR1, which gives this derivative potential to inhibit listed enzymes. According to the results obtained in both docking programs, derivatives **1**, **16**, **17** and **20** could be underlined as the most promising candidates that could be used as anticancer drugs for the therapy of MDR tumors.

## CONCLUSION

Two docking programs (AutoDock Vina and OEDocking) were used for the estimation of binding of twenty designed thiourea derivatives of naproxen to four selected protein kinases involved in tumor multidrug resistance (MDR). According to OEDocking, the highest potential to inhibit these enzymes have derivatives **1** (inhibition of AKT2 and mTOR) and **20** (inhibition of EGFR and VEGFR1). According to AutoDock Vina, the highest potential to inhibit EGFR, AKT2 and VEGFR1 have derivatives **16** and **17**. Derivatives **1**, **16**, **17** and **20** are the most promising candidates that could be used for the therapy of MDR tumors.

## ACKNOWLEDGEMENTS

This work was supported by the Faculty of Medical Sciences University of Kragujevac (Junior Project No. 11/20).

## CONFLICTS OF INTEREST

Authors declare that there are no conflicts of interest regarding the publication of this article.

## REFERENCES

1. Angiolillo DJ, Weisman SM. Clinical pharmacology and cardiovascular safety of naproxen. Am J Cardiovasc Drugs. 2017;17(2):97-107.
2. Moore N, Scheiman JM. Gastrointestinal safety and tolerability of oral non-aspirin over-the-counter analgesics. Postgrad Med J. 2018;130(2):188-99.
3. Katritzky AR, Jishkariani D, Narindoshvili T. Convenient synthesis of ibuprofen and naproxen aminoacyl, dipeptidoyl and ester derivatives. Chem Biol Drug Des. 2009;73(6):618–26.
4. Piffar P, Fernandez R, Tchaikovski O Jr, Hirabara SM, Folador A, Pinto GJ, et al. Naproxen, clenbuterol and insulin administration ameliorates cancer cachexia and reduce tumor growth in Walker 256 tumor-bearing rats. Cancer Lett. 2003;201(2):139–48.
5. Chen PC, Patil V, Guerrant W, Green P, Oyelere AK. Synthesis and structure–activity relationship of histone deacetylase (HDAC) inhibitors with triazole-linked cap group. Bioorg Med Chem. 2008;16(9): 4839–53.
6. Khalifa MM, Ismail MM, Eissa S, Ammar Y. Design and synthesis, of some novel 6-methoxynaphthalene derivatives with potential anticancer activity. Der Pharma Chem. 2012;4(4):1552–66.
7. Kumar V, Chimni SS. Recent developments on thiourea based anticancer chemotherapeutics. Anti-Cancer Agents Med Chem. 2015;15(2):163-75.
8. Prajapati NP, Patel HD. Novel thiosemicarbazone derivatives and their metal complexes: Recent development. Synth Commun. 2019;49(21):2767-804.
9. Lourenco AL, Saito MS, Dorneles LE, Viana GM, Sathler PC, Aguiar LC, et al. Synthesis and antiplatelet activity of antithrombotic thiourea compounds: biological and structure-activity relationship studies. Molecules. 2015;20(4):7174-200.
10. Liu W, Zhou J, Zhang T, Zhu H, Qian H, Zhang H, et al. Design and synthesis of thiourea derivatives containing a benzo[5,6]cyclohepta[1,2-b]pyridine moiety as potential antitumor and anti-inflammatory agents. Bioorg Med Chem Lett. 2012;22:2701-4.
11. Shakeel A. Thiourea Derivatives in Drug Design and Medicinal Chemistry: A Short Review. J Drug Des Med Chem. 2016;2:10.
12. Hu H, Lin C, Ao M, Ji Y, Tang B, Zhou X, et al. Synthesis and biological evaluation of 1-(2-(adamantane-1-yl)-1H-indol-5-yl)-3-substituted urea/thiourea derivatives as anticancer agents. RSC Adv. 2017;7:51640-51.
13. Pingaew R, Sinthupoom N, Mandi P, Prachayasittikul V, Cherdtrakulkiat R, Prachayasittikul S, et al. Synthesis, biological evaluation and in silico study of bis-thiourea derivatives as anticancer, antimalarial and antimicrobial agents. Med Chem Res. 2017;26:3136-48.
14. Zhang H, Zhang Y, Wu G, Zhou J, Huang W, Hu X. Synthesis and biological evaluation of sulfonylurea and thiourea derivatives substituted with benzenesulfonamide groups as potential hypoglycemic agents. Bioorg Med Chem Lett. 2009;19:1740-4.
15. Nordin NA, Chai TW, Tan BL, Choi CL, Abd Halim AN, Hussain H, et al. Novel synthetic monothiourea aspirin derivatives bearing alkylated amines as potential antimicrobial agents. J Chem. 2017;2017.
16. Li J, Tan JZ, Chen LL, Zhang J, Shen X, Mei CL, et al. Design, synthesis and antitumor evaluation of a new series of *N*-substituted-thiourea derivatives 1. Acta Pharmacol Sin. 2006;27(9):1259-71.
17. Lu PC, Li HQ, Sun J, Zhou Y, Zhu HL. Synthesis and biological evaluation of pyrazole derivatives containing thiourea skeleton as anticancer agents. Bioorg Med Chem. 2010;18(13):4606-14.

18. Yao J, Chen J, He Z, Sun W, Xu W. Design, synthesis and biological activities of thiourea containing sorafenib analogs as antitumor agents. Bioorg Med Chem. 2012;20(9):2923-9.
19. Li HQ, Yan T, Yang Y, Shi L, Zhou CF, Zhu HL. Synthesis and structure–activity relationships of *N*-benzyl-*N*-(X-2-hydroxybenzyl)-*N*′-phenylureas and thioureas as antitumor agents. Bioorg Med Chem. 2010;18:305-13.
20. Zhao Y, Wang C, Wu Z, Fang J, Zhu L. Synthesis and antitumor activity of novel aroylthiourea derivatives of podophyllotoxin. Invest New Drugs. 2012;30:17-24.
21. Moeker J, Teruya K, Rossit S, Wilkinson BL, Lopez M, Bornaghi LF, et al. Design and synthesis of thiourea compounds that inhibit transmembrane anchored carbonic anhydrases. Bioorg Med Chem. 2012;20(7):2392-404.
22. Huhtiniemi T, Suuronen T, Rinne VM, Wittekindt C, Kakkonen ML, Jarho E, et al; Leppanen, J. Oxadiazole-carbonylaminothioureas as SIRT1 and SIRT2 inhibitors. J Med Chem. 2008;51:4377-80.
23. Gagic Z, Ruzic D, Djokovic N, Djikic T, Nikolic K. In silico Methods for Design of Kinase Inhibitors as Anticancer Drugs. Front Chem. 2020;7:873.
24. Ferguson FM, Gray NS. Kinase inhibitors: the road ahead. Nat Rev Drug Discov. 2018;17(5):353-77.
25. Akhtar MJ, Siddiqui AA, Khan AA, Ali Z, Dewangan RP, Pasha S, et al. Design, synthesis, docking and QSAR study of substituted benzimidazole linked oxadiazole as cytotoxic agents, EGFR and erbB2 receptor inhibitors. Eur J Med Chem. 2017;126:853-69.
26. Luqmani YA. Mechanisms of drug resistance in cancer chemotherapy. Med Princ Pract. 2005;14:35–48.
27. Wu Q, Yang Z, Nie Y, Shi Y, Fan D. Multi-drug resistance in cancer chemotherapeutics: Mechanisms and lab approaches. Cancer Lett. 2014;347:159–66.
28. Wang X, Zhang H, Chen X. Drug resistance and combating drug resistance in cancer. Cancer Drug Resist. 2019;2:141–160.
29. Dallavalle S, Dobričić V, Lazzarato L, Gazzano E, Machuqueiro M, Pajeva I, et al. Improvement of conventional anti-cancer drugs as new tools against multidrug resistant tumors. Drug Resist Updat. 2020; 50: 100682.
30. Jin Y, Zhang W, Xu J, Wang H, Zhang Z, Chu C, et al. UCH-L1 involved in regulating the degradation of EGFR and promoting malignant properties in drug-resistant breast cancer. Int J Clin Exp Pathol. 2015;8(10):12500–8.
31. To KK, Poon DC, Wei Y, Wang F, Lin G, Fu LW. Vatalanib sensitizes ABCB1 and ABCG2-overexpressing multidrug resistant colon cancer cells to chemotherapy under hypoxia. Biochem pharmacol. 2015;97(1):27-37.
32. Liu R, Chen Y, Liu G, Li C, Song Y, Cao Z, et al. PI3K/AKT pathway as a key link modulates the multidrug resistance of cancers. Cell Death Dis. 2020;11(9):1-2.
33. Knuefermann C, Lu Y, Liu B, Jin W, Liang K, Wu L, et al. HER2/PI-3K/Akt activation leads to a multidrug resistance in human breast adenocarcinoma cells. Oncogene. 2003;22(21):3205-12.
34. ChemOffice Ultra 7.0.1, 2002, CambridgeSoft Corporation, Cambridge, MA, USA (http://www.cambridgesoft.com).
35. Morris GM, Huey R, Lindstrom W, Sanner MF, Belew RK, Goodsell DS, et al. AutoDock4 and AutoDockTools4: Automated docking with selective receptor flexibility. J Comput Chem. 2009;30(16): 2785-91.
36. OMEGA 2.5.1.4: OpenEye Scientific Software, Santa Fe, NM. http://www.eyesopen.com/.
37. Hawkins PCD, Skillman AG, Warren GL, Ellingson BA, Stahl MT. Conformer Generation with OMEGA: Algorithm and Validation Using High Quality Structures from the Protein Databank and the Cambridge Structural Database. J Chem Inf Model. 2010;50:572-84.
38. BIOVIA, Dassault Systèmes, Discovery Studio Visualizer, 17.2.0.16349, San Diego: Dassault Systèmes, 2016.
39. MAKE Receptor 3.2.0.2: OpenEye Scientific Software, Santa Fe, NM. https://www.eyesopen.com/.
40. Trott O, Olson AJ. AutoDock Vina: improving the speed and accuracy of docking with a new scoring function, efficient optimization, and multithreading. J comput chem. 2010;31(2):455-61.
41. FRED 3.2.0.2: OpenEye Scientific Software, Santa Fe, NM. https://www.eyesopen.com/.
42. McGann M. FRED pose prediction and virtual screening accuracy. J Chem Inf Model. 2011;51:578-96.
43. McGann M. FRED and HYBRID docking performance on standardized datasets. J Comput Aided Mol Des. 2012; 26: 897-906.
44. Macrae CF, Edgington PR, McCabe P, Pidcock E, Shields GP, Taylor R, et al. Mercury: visualization and analysis of crystal structures. J Appl Crystallogr. 2006;39(3):453-7.
45. Protein Data Bank available at http://www.rcsb.org/
46. Carugo O, Pongor S. A normalized root-mean-spuare distance for comparing protein three-dimensional structures. Protein Sci. 2001;10(7):1470-3.
47. Stamos J, Sliwkowski MX, Eigenbrot C. Structure of the epidermal growth factor receptor kinase domain alone and in complex with a 4-anilinoquinazoline inhibitor. J Biol Chem. 2002;277(48):46265-72.
48. Widiandani T, Siswandono S, Meiyanto E, Sulistyowaty MI, Purwanto BT, Hardjono S. New N-allylthiourea derivatives: synthesis, molecular docking and in vitro cytotoxicity studies. Trop J Pharm Res. 2018;17(8):1607-13.
49. Rouse MB, Seefeld MA, Leber JD, McNulty KC, Sun L, Miller WH, et al. Aminofurazans as potent inhibitors of AKT kinase. Bioorg Med Chem Lett. 2009;19(5):1508-11.
50. Yang H, Rudge DG, Koos JD, Vaidialingam B, Yang HJ, Pavletich NP. mTOR kinase structure, mechanism and regulation. Nature. 2013;497(7448):217-23.